THE DROP OF THE COHERENCE OF THE LOWER KILOHERTZ QUASI-PERIODIC BRIGHTNESS VARIATIONS IS ALSO OBSERVED IN XTE J1701−462

D. Barret[1,2], M. Bachetti[1,2], and M. Coleman Miller[3,4]

[1] Université de Toulouse (UPS), 9 av. du Colonel Roche, 31028 Toulouse Cedex 9, France; didier.barret@cesr.fr
[2] Centre National de la Recherche Scientifique, Centre d'Etude Spatiale des Rayonnements, UMR 5187, 9 av. du Colonel Roche, BP 44346, 31028 Toulouse Cedex 4, France
[3] Department of Astronomy and Maryland Astronomy Center for Theory and Computation, University of Maryland, College Park, MD 20742-2421, USA

ABSTRACT

We investigate the quality factor and root mean square (rms) amplitude of the lower kilohertz quasi-periodic brightness variations (kHz QPOs) from XTE J1701−462, a unique X-ray source which was observed in both the so-called Z and atoll states. Correcting for the frequency drift of the QPO, we show that, as in all sources for which such a correction can be applied, the quality factor and rms amplitude drops sharply above a critical frequency. For XTE J1701−462, this frequency is estimated to be ∼800 Hz, where the quality factor reaches a maximum of ∼200 (e.g., a value consistent with the one observed from more classical systems, such as 4U 1636−536). Such a drop has been interpreted as the signature of the innermost stable circular orbit, and that interpretation is consistent with the observations we report here. The kHz QPOs in the Z state are much less coherent and lower amplitude than they are in the atoll state. We argue that the change of the QPO properties between the two source states is related to the change of the scale height of the accretion disk; a prediction of the toy model proposed by Barret et al. As a by-product of our analysis, we also increased the significance of the upper kHz QPO detected in the atoll phase up to 4.8σ (single trial significance) and show that the frequency separation (266.5 ± 13.1 Hz) is comparable with the one measured from simultaneous twin QPOs in the Z phase.

Key words: accretion, accretion disks – stars: individual (XTE J1701−462) – X-rays: binaries – X-rays: individual (XTE J1701−462) – X-rays: stars

Online-only material: color figures, machine-readable table

1. INTRODUCTION

Kilohertz quasi-periodic brightness variations (kHz QPOs) have been detected from more than 20 low-mass X-ray binaries containing a weakly magnetized neutron star (van der Klis 2006). A pair of QPOs is often detected, with a frequency separation that typically changes by tens of hertz as the individual QPO frequencies change by hundreds of hertz. In lower luminosity systems (often called atoll sources after the tracks they make in color–color diagrams), the lower frequency QPO can reach quality factors ($Q \equiv \nu/\Delta\nu$) up to 200, whereas the upper kHz QPO is usually a broader feature with maximum Q around 50 (see, e.g., Barret et al. 2005a, 2005b, 2006). In brighter systems (often called Z sources), both the lower and upper kHz QPOs are broader features, with maximum Q of a few tens (Boutelier et al. 2010). In lower luminosity sources, for which the quality factor of the lower kHz QPO can be measured over its entire frequency span after correcting for the frequency drifts, Q increases with frequency until it reaches a maximum around 800–900 Hz, beyond which a sharp drop-off is observed. The presence of the drop in many systems, and its reproducibility in a given system independent of count rate and spectral hardness (Barret et al. 2007), led to the suggestion that it may be related to the existence of an innermost stable circular orbit, a key prediction of strong field general relativity (Barret et al. 2006).

XTE J1701−462 is a unique X-ray source, which first behaved like a Z source at high luminosity, and which later behaved like an atoll source at much lower luminosities. The source was closely monitored with the *RXTE* Proportional

Counter Array (PCA) during its 2006 and 2007 outburst (Homan et al. 2007, 2010; Lin et al. 2009b). Type I X-ray bursts were studied by Lin et al. (2009a). The three bursts observed occurred as the source were in transition from the typical Z-source behavior to the typical atoll-source behavior, at ∼10% of the Eddington luminosity. No significant burst oscillations in the range 30–4000 Hz were found during these three bursts. Lin et al. (2009a) also derive a distance estimate of 8.8 ± 1.3 kpc from two radius expansion bursts (the latter two of the three). In both states, kHz QPOs have been reported, with very different properties, yet following the general trend that in the Z state, QPOs showed lower Q and amplitude than in the atoll state (Homan et al. 2007, 2010; Sanna et al. 2010). The luminosity range over which kHz QPOs are detected between the Z and atoll state spans a factor of 15–20. The dramatic changes in the QPO parameters between the two source states could not be due to changes in the neutron star mass, its magnetic field, its spin, or even the inclination of the accretion disk. It is thus more plausible that they were instead caused by a change in the properties of the accretion flow. This led Sanna et al. (2010) to conclude first that effects other than the geometry of space time around the neutron star have a strong influence on the coherence and amplitude of the kHz QPOs and second that the drop of the coherence and root mean square (rms) amplitude of the lower kHz QPOs, as we have observed it, could not be used to infer the existence of the innermost stable circular orbit around a neutron star.

In this paper, we revisit the *RXTE* observations reported by Sanna et al. (2010), focusing on the lower kHz QPO and apply the same analysis procedures (frequency drift correction) as described in Barret et al. (2006). The main reason is that, despite very few detections overall (12 segments of observations in

[4] Also at Joint Space Science Institute, University of Maryland College Park, MD 20742-2421, USA.

total), the frequency span of the lower kHz QPO ranges from about 640 Hz to 850 Hz, and by comparison with other sources, this should be sufficient to investigate the drop of its quality factor (no such drop is obvious in Figure 3 of Sanna et al. (2010) who used a different analysis than Barret et al. (2006)). In the following section, we describe the re-analysis of the lower kHz QPOs reported by Sanna et al. (2010) to show that the drop of its quality factor and rms amplitude is indeed observed. We then discuss the changes in the properties of the QPOs from XTE J1701−462 as simply related to a likely decrease of the disk thickness between the Z and atoll phases, as previously discussed in the framework of the toy model presented in Barret et al. (2007).

2. OBSERVATIONS

We follow the definition of the Z and atoll states as in Sanna et al. (2010): the separation is estimated around the end of 2007 April. We have retrieved from the HEASARC archive science event mode and single bit data recorded by the *RXTE* PCA. We consider data as segments of continuous observation (an ObsID may contain more than 1 segment). For each segment, we have computed an average Power Density Spectrum (PDS) with a 1 Hz resolution and an integration time of 16 s, using events recorded between 2 and 40 keV. The PDSs are normalized according to Leahy et al. (1983), so that the Poisson noise level is expected to be a constant close to 2. The PDS is then blindly searched for excess power between 500 Hz and 1400 Hz using a scanning technique, as presented in Boirin et al. (2000). We have also verified that no significant excesses were detected between 1400 and 2048 Hz. This justifies the use of the 1400–2048 Hz range to estimate accurately the Poisson noise level in each observation, which is indeed close to 2 in all segments of data.

The excess power is then fitted with a Lorentzian with three free parameters: frequency, full width at half-maximum, and amplitude (equal to the integrated power of the Lorentzian). The Poisson noise level is fitted separately above 1400 Hz. Sixty-eight percent confidence errors on each parameter are computed in a standard way, using a $\Delta\chi^2$ of 1. Following Boutelier et al. (2009), our threshold for QPOs is related to the ratio (hereafter R) of the Lorentzian amplitude to its 1σ error[5] (R was often quoted and used as a significance). A conservative threshold $R = 3$ means that we consider only QPOs for which we can measure the power of the Lorentzian with an accuracy of 3σ or more. Such a threshold corresponds to a $\sim6\sigma$ excess power in the PDS for a single trial, equivalent to $\sim4\sigma$ if we account for the number of trials of the scanning procedure (van der Klis 1989). The integrated power of the Lorentzian is then converted into an rms, expressed as a fraction of the total source count rate.

We detect a significant QPO in 12 segments of observations, within the same ObsIDs as in Sanna et al. (2010). The reduced number of active PCUs on the PCA, and the relative faintness of the source in its atoll phase (count rate between ~40 and ~120 counts s^{-1} PCU^{-1}), means that special care must be

---

5 The Lorentzian function used in the fit is
Lor$(\nu) = A \times W/(2\pi)/[(\nu - \nu_0)^2 + (W/2)^2]$, where A is the integrated power of the Lorentzian from 0 to ∞, W is its width, and ν_0 is its centroid frequency. The fitted function is linear in A, and therefore its error can be computed using $\Delta\chi^2$ (e.g., Press et al. 1992). The rms amplitude is a derived quantity, computed as rms $= \sqrt{A/S}$, where S is the source count rate (van der Klis 1989). In this paper, we have defined $R = A/\delta A$, from which the error on the rms is estimated as δrms $= 1/2 \times$ rms $\times R^{-1}$ after neglecting the term $\delta S/S$ in the derivative of the rms equation.
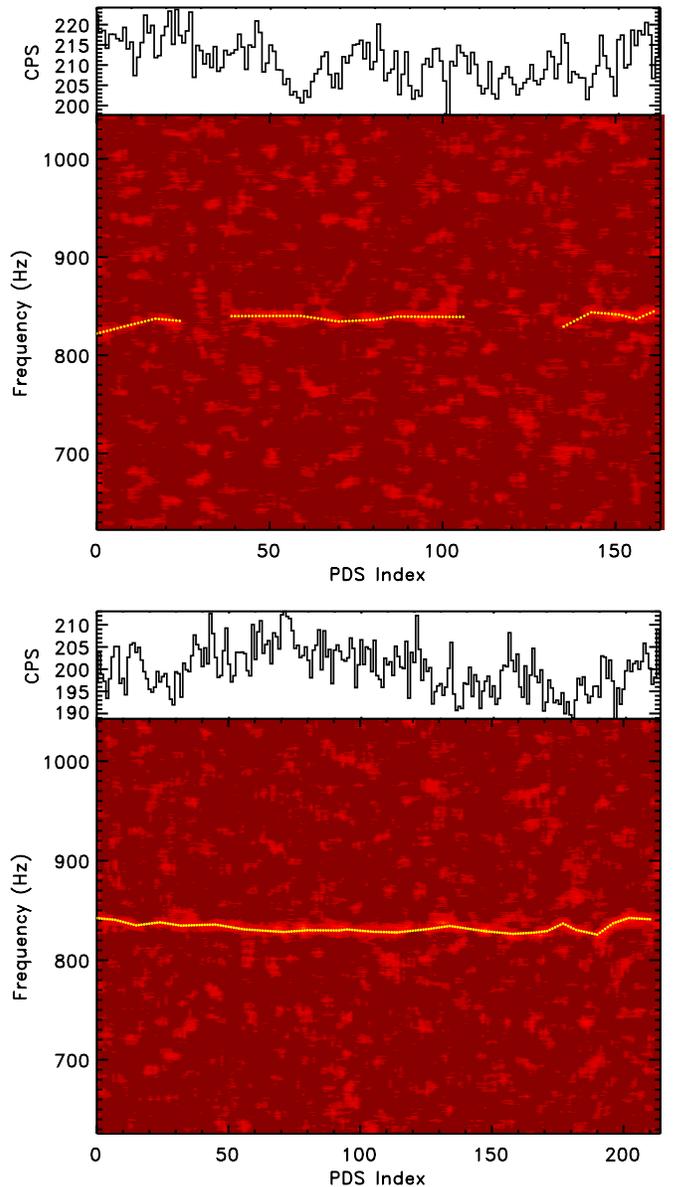

Figure 1. QPO frequency history recovered by our analysis for two segments of observation of the ObsID 93703-01-02-05. The path followed by the QPO is indicated with the yellow filled circles. As can be seen on the left, there are gaps in the QPO detection. When the gap duration is less than 256 s, frequencies within the gap are estimated by interpolating between the two positive detections surrounding the gap.
(A color version of this figure is available in the online journal.)

taken to correct for the frequency drift of the lower kHz QPO. We apply the very same technique as in Barret et al. (2006). It is an iterative procedure, which enables us to bound the QPO frequencies on shorter and shorter integration time, with narrower and narrower frequency intervals. As the integration time decreases, the significance threshold set to the scanning technique (Boirin et al. 2000) is adjusted (e.g., the threshold is decreased from 4σ for an interval of 50 Hz over a few thousand seconds to 3σ for an interval of 10 Hz over a few hundreds of seconds). The QPO path is then recovered through a linear interpolation between the most significant detections with the shortest integration time. An example of the application of the analysis to two segments of real observations is shown in Figure 1.

Table 1
Lower kHz QPOs Detected in the Atoll Phase of XTE J1701−462

Number	ObsID	Date	Time	Duration	C	ν	Qa	rms	R
01	93703-01-02-04	2007 Jul 24	08–44–11	1968	116.9	849.9 ± 0.5	126.2 ± 26.0	7.8 ± 0.6	7.0
02	93703-01-02-04	2007 Jul 24	10–15–27	1280	117.3	854.2 ± 0.7	105.7 ± 24.6	8.7 ± 0.7	6.3
03	93703-01-02-05	2007 Jul 25	10–02–49	1920	105.8	837.5 ± 0.3	138.3 ± 24.3	9.5 ± 0.5	8.8
04	93703-01-02-05	2007 Jul 25	11–23–27	3376	66.7	832.9 ± 0.2	152.2 ± 13.2	8.8 ± 0.3	16.0
05	93703-01-02-08	2007 Jul 25	13–14–40	2304	104.9	835.4 ± 0.2	176.5 ± 21.8	9.1 ± 0.4	11.0
06	93703-01-02-11	2007 Jul 25	05–13–35	2528	108.2	834.9 ± 0.3	175.1 ± 31.5	7.7 ± 0.5	8.1
07	93703-01-02-11	2007 Jul 25	06–40–31	3392	68.1	802.8 ± 0.1	189.9 ± 13.1	9.4 ± 0.2	20.4
08	93703-01-02-11	2007 Jul 25	08–14–23	208	71.0	786.7 ± 0.4	168.7 ± 37.2	10.3 ± 0.8	6.3
09	93703-01-03-00	2007 Jul 29	03–19–30	3344	56.4	772.7 ± 0.8	94.3 ± 24.8	10.5 ± 0.9	5.6
10	93703-01-03-00	2007 Jul 29	04–53–19	3408	39.2	712.1 ± 0.6	71.3 ± 9.4	11.4 ± 0.6	9.7
11	93703-01-03-00	2007 Jul 29	06–27–27	2976	42.1	707.7 ± 0.4	103.4 ± 17.1	10.3 ± 0.6	9.1
12	93703-01-03-02	2007 Jul 29	11–23–57	1360	39.7	655.1 ± 1.0	73.6 ± 19.3	9.9 ± 1.0	5.2

Notes. Parameters are averaged over the segments of observation, after aligning all the PDSs to a reference frequency. The table lists the segment number, the ObsID name, the date, the duration of the segment, the mean count rate normalized by the number of active PCUs, the reference frequency of the QPO, its quality factor, its rms amplitude, and the accuracy R ratio, as defined in the text.

Such a technique, which we have used extensively on real and simulated data, is able to correct precisely for the frequency drift of QPOs of the strength reported here. In those simulations, the QPO frequency evolution is modeled by a random walk of a given step (e.g., 0.2–0.5 Hz s^{-1}). We follow Timmer & Koenig (1995) and generate synthetic 1 s PDS, for which the underlying model consists of a constant (2) to account for the Poisson noise plus a Lorentzian to model the QPO profile, with parameters (Q and rms) appropriate for each frequency (estimated from the random walk). The simulated PDSs are then combined on (16 s timescales) and scanned as the real data to recover the time evolution of the QPO frequency and to determine Q and rms, for comparison with the parameters injected in the simulations. The difference between the reconstructed and original Q and rms parameters can then be evaluated. Those simulations have shown that for QPOs of comparable strength to the one of XTE J1701−462 (mean rms around 9%), Q can be recovered with an accuracy better than 10% (the accuracy on the rms is better than a few %).

Having reconstructed the QPO frequency evolution, one can compute the mean QPO parameters over the observations, by aligning all the 16 s PDSs for which a QPO frequency was estimated, directly from a significant detection or by interpolation between two significant detections, separated by less than 256 s (see Figure 1). Increasing the latter value to say, 512 s, does not lead to any changes in the fitted QPO parameters. The best-fit results are listed in Table 1 and presented in Figure 2. All the QPOs reported have an $R > 5$ and are therefore highly significant. As can be seen from Figure 2, despite some scatter, there is already evidence that above 800 Hz the quality factor and the rms amplitude of the QPO drops.

In addition to those highly significant QPOs, we also note that there are hints for two additional single QPOs in the segments 93703-01-03-04 and 93703-01-05-06. No frequency drift corrections are possible for those two QPOs. In the first segment, $\nu = 905.0 \pm 4.4$ Hz, $Q = 40.6 \pm 19.3$ for an R ratio of 2.9, while in the second one $\nu = 548.3 \pm 33.2$, $Q = 2.7 \pm 1.6$ for an R factor of 2.3. Being single and not very significant, it is difficult to draw any firm conclusions. However, it cannot be excluded that they are lower kHz QPOs, extending on both sides the frequency span of Figure 2, in which case one would expect them to have low Q factors, as measured (with indeed the caveat that no drift correction could be applied, implying that the measured values are only lower limits on Q).
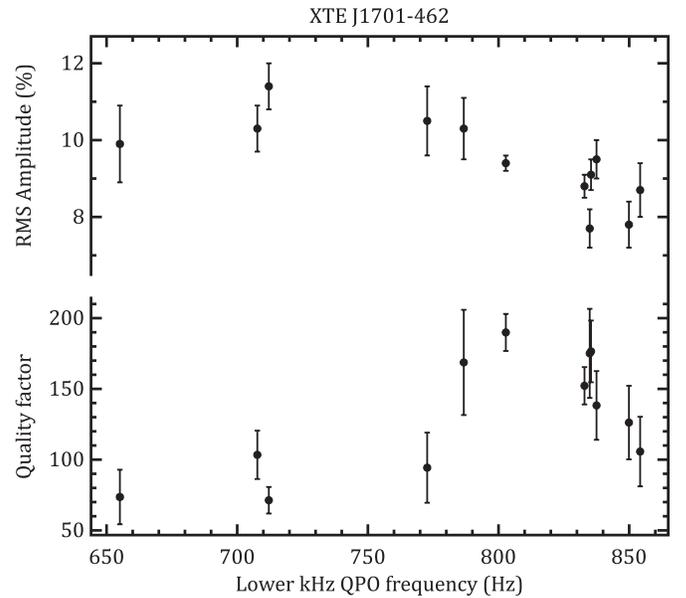

Figure 2. RMS amplitude (top panel) and quality factor (bottom panel) of the lower kHz QPO from XTE J1701−462 as averaged over the 12 segments of observations. There is a trend for the quality factor and the rms amplitude to decrease after reaching a maximum around 800 Hz, in a very similar way as observed in other sources.

The histogram of interpolated frequencies (measured over 16 s) is shown in Figure 3; the full list of detections is available as an online table, while, as an example, a list of the first ten detections is available in Table 2. As can be seen, the frequency span of the lower QPO, although comparable in breadth with other systems, has not been sampled equally (there is a lack of observations around 750 Hz). Grouping the data over constant frequency intervals is therefore not the optimum way to proceed. Instead we have considered adjacent frequency intervals of varying widths, each including 200 QPO frequencies, allowing a better sampling of the peak of the quality factor versus frequency curve. The result is shown in Figure 4. As can be seen, the drops around 800 Hz of the QPO rms amplitude and quality factor are now much clearer and have significantly less scatter. Thanks to our QPO tracking procedure, we can recover the QPO frequency on a timescale of 16 s, whereas Sanna et al. (2010) averaged as many 16 s PDSs as required to enable a significant detection. This explains why on average we get larger Q factors

Table 2
Online Table of QPO Frequency Data Used in Table 1 (Only the First 10 Rows are Shown)

Year	Month	Day	Hour	Minute	Second	Starting Date (s)	Stoping Date (s)	Frequency (Hz)
2007	Jul	24	08	43	24	427884204	427884220	840.684
2007	Jul	24	08	43	40	427884220	427884236	840.554
2007	Jul	24	08	43	56	427884236	427884252	840.423
2007	Jul	24	08	44	12	427884252	427884268	840.293
2007	Jul	24	08	44	28	427884268	427884284	840.163
2007	Jul	24	08	44	44	427884284	427884300	840.033
2007	Jul	24	08	45	00	427884300	427884316	839.903
2007	Jul	24	08	45	16	427884316	427884332	839.773
2007	Jul	24	08	45	32	427884332	427884348	839.643
2007	Jul	24	08	45	48	427884348	427884364	839.513
⋯	⋯	⋯	⋯	⋯	⋯	⋯	⋯	⋯

Notes. The calendar dates of the start (the first six columns), the starting (Column 7), and stopping (Column 8) dates given in elapsed seconds since 1994 January 1 are given for each PDS segment (16 s long), together with the estimated QPO frequency (Column 9).

(This table is available in its entirety in a machine-readable form in the online journal. A portion is shown here for guidance regarding its form and content.)
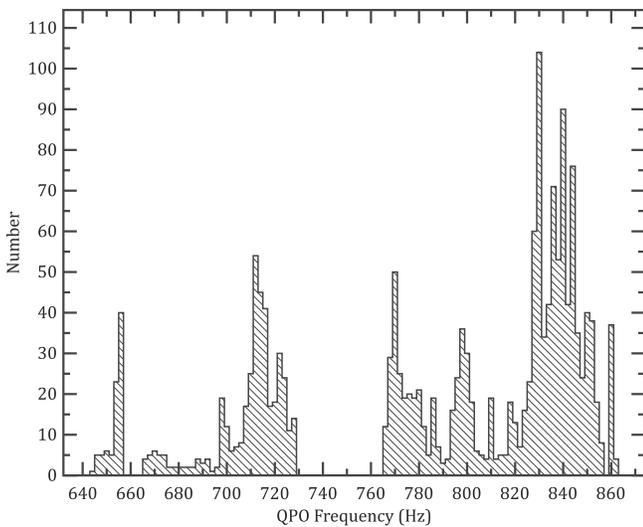

Figure 3. Histogram of the frequencies (one frequency per 16 s) detected in all 12 observations, showing that not all frequencies have been sampled equally. The frequencies used for building the histogram are available in an online table (see Table 2 for the first 10 rows).
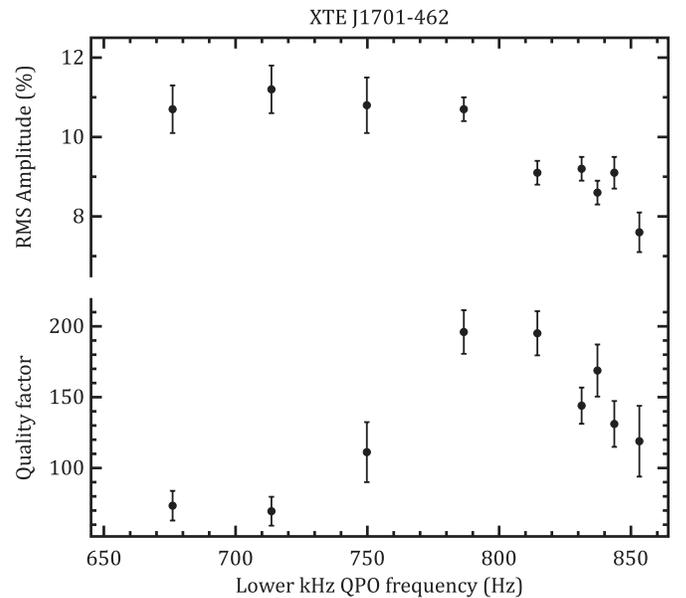

Figure 4. Same as Figure 2, but the QPO parameters are averaged over frequency intervals (200 consecutive frequencies were combined). The drop in Q and rms amplitudes is now clearer.

than Sanna et al. (2010) and hence a better description of its frequency dependence.

Following Sanna et al. (2010), we have shifted all the 16 s PDSs to search for the upper kHz QPO. Sanna et al. (2010) reported a 3.1σ significance detection (single trial) with a frequency separation of 258 ± 13 Hz. Using our procedure, the significance of the upper kHz QPO detected rises to 4.8σ (single trial significance), for a frequency separation of 266.5 ± 13.1 Hz, consistent with the value of Sanna et al. (2010). At the same time, the significance of the main peak increased from 30σ to more than 50σ in our analysis (see Figure 5). In the two ObsIDs of the Z phase, in which the simultaneous twin kHz QPOs are the most significant ($R \geqslant 3$; 92405-01-40-04 and 92405-01-40-05), we have measured a frequency difference of 280.8 ± 17.6 and 276.1 ± 18.8 Hz, respectively, i.e., consistent within errors with the frequency difference we have measured in the atoll phase.

3. DISCUSSION

Based on the observations reported here, our main findings can be summarized as follows.

1. XTE J1701−462 behaves similarly to the other sources we have studied. In the atoll state, its lower kHz QPOs are narrow. Correcting for the frequency drift, we have been able to show that its quality factor reaches a maximum of 200 around 800 Hz before dropping off sharply. This effect is even visible within a limited sample of observations, when the drift correction is applied. We have also found a weaker upper kHz QPO with a significance greater than previously reported, using the shift-and-add technique.

2. Following Barret et al. (2006), we estimate the frequency at the ISCO by adding $\sim$270 Hz $\nu_{\mathrm{lower},Q=0}$, which we infer to be around 900 Hz (albeit with large uncertainty due to the limited sample of the Q–ν curve in the available data set). This gives $\nu_{\mathrm{ISCO}} \approx 1170$ Hz. No upper QPO above that frequency should be detected in XTE J1701−462. This is consistent with the findings of Sanna et al. (2010), who reported upper QPOs with frequencies less than $\sim$930 Hz. From ν_{ISCO}, we can estimate the gravitational masses of the
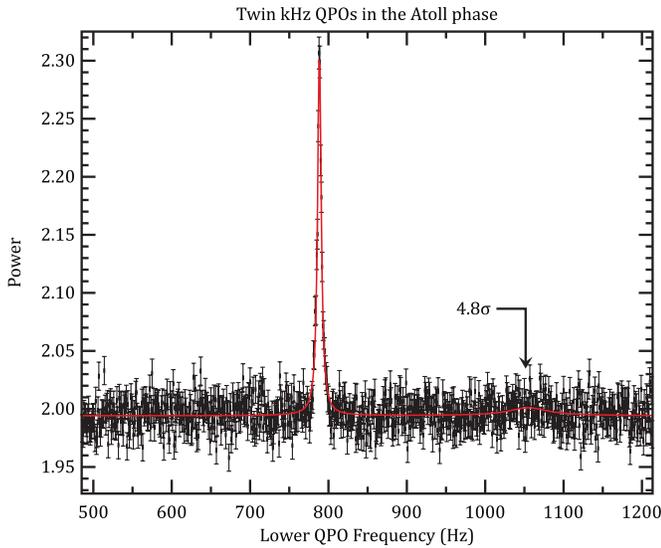
Figure 5. Two kHz QPOs detected by shifting and adding all the 16 s PDSs in which a QPO frequency could be estimated. The main peak has a significance above 50σ, whereas the upper kHz QPO has a single trial significance of 4.8σ. Its quality factor is 17.1 ± 9.1 and its rms amplitude is 4.4 ± 0.8, and its R ratio is 2.6.

(A color version of this figure is available in the online journal.)

neutron stars (Miller et al. 1998):

$$M \approx 2.2\, M_\odot (1000\,\mathrm{Hz}/\nu_{\mathrm{ISCO}})(1 + 0.75\,j), \qquad (1)$$

where $j \equiv cJ/(GM^2) \sim 0.1$–$0.2$ is the dimensionless angular momentum of the star. The inferred mass of the neutron star in XTE J1701−462 would therefore be $\sim 2.0\, M_\odot$.

3. As shown by Sanna et al. (2010), when the source is in the Z phase, the properties of its QPOs are consistent with those observed in other Z sources: they are weak and broad (the maximum Q values are about 10 and the rms less than $\sim 4\%$). For the purpose of this paper, we have also re-analyzed the segments of data in which Sanna et al. (2010) reported a QPO, and our results are globally consistent with theirs. Note, however, that no frequency drift corrections can be applied when recovering the quality factor, hence the measured values should be considered as lower limits. In any case, our independent analysis confirms that no highly coherent QPOs have been detected from XTE J1701−462 in the Z phase. This indeed suggests that there is a parameter which alters the Q value, in addition to the radius at which the QPOs originate. Sanna et al. (2010) conclude that these results weaken the hypothesis relating the drop in coherence observed in many sources, and in the atoll phase of the one under investigation, to the presence of the ISCO, because there are evidently other properties of the accretion flow that can change the quality factor of QPOs. We point out, though, that the drop in coherence that we relate to the ISCO is a very characteristic phenomenon. In a given source, it happens always at the same frequency, at the higher end of the frequency range of kHz QPOs. There is therefore a significant difference between the drop in coherence we relate to the ISCO and the change in coherence in the different states of this source. In our opinion, this implies that different phenomena are producing the two effects.

Let us now discuss some possible interpretations. The change in coherence of the kHz QPOs in XTE J1701−462 between the atoll and Z phase has to be related to a global change of the accretion configuration.

In the framework of the toy model proposed by Barret et al. (2007), we argue that the difference is related to the scale height of the disk, exactly the same process that we propose as responsible for the general difference in coherence between QPOs in atoll and Z sources. Consistent with this idea, standard disk accretion theory suggests that at rates approaching Eddington (which is expected in the Z state) the disk half-thickness at its inner edge will be comparable to the orbital radius there (Shakura & Sunyaev 1973) and that as a consequence the inward radial drift speed (which scales as $(h/r)^2$, where h is the disk half-thickness) will be large as well. As discussed in Barret et al. (2006), a large inward speed will necessarily decrease Q regardless of other factors. It is therefore not surprising that high luminosity sources have lower Q, as observed (Méndez 2006).

We note that alternative explanations are under study through three-dimensional MHD simulations that show oscillations promisingly similar to the kHz QPOs (for a recent discussion, see Bachetti et al. 2010). In these simulations, the lower and upper kHz QPOs are emitted from hotspots on the surface of the star, produced by streams of matter originating, respectively, from the funnel flow around the magnetic pole and from instabilities at the inner edge of the disk. The properties of these QPOs in simulated systems with an enhanced variety of physical inputs (including different configurations of the disk) are currently under study.

4. CONCLUSIONS

The source XTE J1701−462, which has been observed in both the atoll and Z phases, gives us a unique opportunity to explore the relation between frequency and quality factor. This relation has been claimed for previous atoll sources to provide evidence of the innermost stable circular orbit. It was expected, however, that for higher-luminosity sources, in which the disk becomes geometrically thick and the inward radial speed is thus large, the quality factors would be systematically lower than they are in the lower luminosity atoll sources, as observed (Méndez 2006). XTE J1701−462 does show exactly this behavior. In the atoll state, its Q versus ν phenomenology is consistent with that of other sources, but in the Z state the quality factors are systematically smaller than in the atoll state. The change is over the whole range of the QPO frequencies and is unlike the abrupt drop observed in the atoll phase, which only happens at the higher end of the frequency range. As a consequence, we do not agree with Sanna et al. (2010) that the different coherence in the atoll and Z phases of XTE J1701−462 weakens the ISCO hypothesis.

We can ask: what behavior would contradict the ISCO picture? As discussed in other papers (e.g., Barret et al. 2007), there are several possibilities including (1) a lower or upper kHz QPO frequency in another state that is significantly larger than the projected maximum due to the ISCO, (2) a peak in Q followed by a sharp drop at a frequency significantly less than seen in the atoll state, or (3) a peak in Q followed by a sharp drop in any source at a frequency that would imply an unreasonable ISCO frequency (e.g., below 800 Hz). None of these have yet been seen. Therefore, although the importance of the implications demand further critical analysis, the interpretation is still consistent with all existing data to date.

REFERENCES

Bachetti, M., Romanova, M. M., Kulkarni, A., Burderi, L., & di Salvo, T. 2010, MNRAS, 403, 1193
Barret, D., Kluźniak, W., Olive, J. F., Paltani, S., & Skinner, G. K. 2005a, MNRAS, 357, 1288
Barret, D., Olive, J., & Miller, M. C. 2005b, MNRAS, 361, 855
Barret, D., Olive, J., & Miller, M. C. 2006, MNRAS, 370, 1140
Barret, D., Olive, J., & Miller, M. C. 2007, MNRAS, 376, 1139
Boirin, L., Barret, D., Olive, J. F., Bloser, P. F., & Grindlay, J. E. 2000, A&A, 361, 121
Boutelier, M., Barret, D., Lin, Y., & Török, G. 2010, MNRAS, 401, 1290
Boutelier, M., Barret, D., & Miller, M. C. 2009, MNRAS, 399, 1901
Homan, J., et al. 2007, ApJ, 656, 420
Homan, J., et al. 2010, ApJ, 719, 201
Leahy, D. A., Darbro, W., Elsner, R. F., Weisskopf, M. C., Kahn, S., Sutherland, P. G., & Grindlay, J. E. 1983, ApJ, 266, 160
Lin, D., Altamirano, D., Homan, J., Remillard, R. A., Wijnands, R., & Belloni, T. 2009a, ApJ, 699, 60
Lin, D., Remillard, R. A., & Homan, J. 2009b, ApJ, 696, 1257
Méndez, M. 2006, MNRAS, 371, 1925
Miller, M. C., Lamb, F. K., & Psaltis, D. 1998, ApJ, 508, 791
Press, W. H., Teukolsky, S. A., Vetterling, W. T., & Flannery, B. P. 1992, in Numerical Recipes in FORTRAN, The Art of Scientific Computing, ed. W. H. Press et al. (Cambridge: Cambridge Univ. Press), 654
Sanna, A., et al. 2010, MNRAS, 408, 622
Shakura, N. I., & Sunyaev, R. A. 1973, A&A, 24, 337
Timmer, J., & Koenig, M. 1995, A&A, 300, 707
van der Klis, M. 1989, in Timing Neutron Stars, ed. H. Ögelman & E. P. J. van den Heuvel (New York, NY: Kluwer Academic/Plenum), 27
van der Klis, M. 2006, in Rapid X-ray Variability, ed. W. H. G. Lewin & M. van der Klis (Cambridge: Cambridge Univ. Press), 39